NREL
NATIONAL RENEWABLE ENERGY LABORATORY

An Examination of 1D Solar Cell Model Limitations Using 3D SPICE Modeling

Preprint

W.E. McMahon, J.M. Olson, J.F. Geisz,
and D.J. Friedman

Presented at the 2012 IEEE Photovoltaic Specialists Conference
Austin, Texas
June 3–8, 2012

NREL is a national laboratory of the U.S. Department of Energy, Office of Energy Efficiency & Renewable Energy, operated by the Alliance for Sustainable Energy, LLC.

Conference Paper
NREL/CP-5200-54133
June 2012

Contract No. DE-AC36-08GO28308

NOTICE

Available electronically at http://www.osti.gov/bridge

Available for a processing fee to U.S. Department of Energy
and its contractors, in paper, from:

U.S. Department of Energy
Office of Scientific and Technical Information

P.O. Box 62
Oak Ridge, TN 37831-0062
phone: 865.576.8401
fax: 865.576.5728
email: mailto:reports@adonis.osti.gov

Available for sale to the public, in paper, from:

U.S. Department of Commerce
National Technical Information Service
5285 Port Royal Road
Springfield, VA 22161
phone: 800.553.6847
fax: 703.605.6900
email: orders@ntis.fedworld.gov
online ordering: http://www.ntis.gov/help/ordermethods.aspx

Cover Photos: (left to right) PIX 16416, PIX 17423, PIX 16560, PIX 17613, PIX 17436, PIX 17721

Printed on paper containing at least 50% wastepaper, including 10% post consumer waste.

An Examination of 1D Solar Cell Model Limitations Using 3D SPICE Modeling

W.E. McMahon, J.M. Olson, J.F. Geisz, and D.J. Friedman

National Renewable Energy Laboratory, Golden, CO, 80401, USA

***Abstract* — To examine the limitations of one-dimensional (1D) solar cell modeling, 3D SPICE-based modeling is used to examine in detail the validity of the 1D assumptions as a function of sheet resistance for a model cell. The internal voltages and current densities produced by this modeling give additional insight into the differences between the 1D and 3D models.**

***Index Terms* — current-voltage characteristics, photovoltaic cells, semiconductor device modeling, SPICE**

I. Introduction

One-dimensional (1D) solar cell modeling can do an excellent job of representing actual cell behavior over a wide range of conditions. By definition, a 1D model assumes that diode voltages and current densities are spatially uniform in the plane of the cell, for every layer in the cell. These assumptions are generally a good approximation for a well-designed cell under "normal" operating conditions with uniform illumination, and a 1D model, therefore, works well for designing and modeling cells under most conditions. However, the 1D model assumptions begin to fail when the lateral current transport in the resistive layers of a solar cell requires a non-negligible lateral voltage, which in turn causes a spatial variation in the diode voltage and current density of the adjacent junctions.

Three-dimensional modeling based on the SPICE circuit solver [1] offers an alternative to 1D modeling, and is being used for cell modeling of explicitly non-uniform conditions such as non-uniform irradiance [2, 3], chromatic aberration (for multijunction cells) [2, 4], or perimeter recombination [5]. It can also be used to model forward biasing during dark-IV measurements [5], or to model high concentrations during either operation or characterization [6]. The common theme for all of these situations is that the cell is operating in a regime where the 1D assumptions of uniform diode voltage and current density are beginning to fail. Here we use 3D modeling based on SPICE (Simulation Program with Integrated Circuit Emphasis) to examine in detail the failure of 1D assumptions as a function of sheet resistance for a model cell.

II. Computational Method

A 3D SPICE-based model is used in which a solar cell is represented by a 3D network of diodes, resistors, and current sources. SPICE then generates an I-V curve for this equivalent circuit. To do so, it solves for the voltage at each node in the resulting circuit over a range of load voltages. Analysis of these internal voltages often provides additional insight in the cell's operation.

This type of modeling is becoming more common [2, 6-8] and is well described in Ref. [6]. In this study, we used MacSPICE [9] for the circuit convergence. Other versions of SPICE or related algorithms [8] can also be used.

The cell geometry and cell parameters used for calculations are shown in Fig. 1. Photocurrent is uniformly generated over the entire illuminated area and collected by two (opaque) top contacts. This configuration was chosen to illustrate two aspects of a real cell: (1) optical obscuration of a fraction of the total cell area by a top contact, and (2) current transport across a lateral-conduction layer (LCL) to a grid finger. In order to focus on these two cell features in isolation, transport along grid fingers has been omitted and contact resistances have

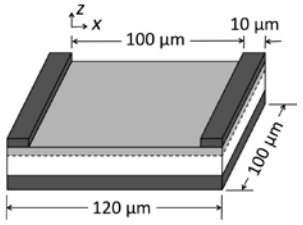

Fig. 1. Cell geometry used for calculations. Diode parameters for the junction (dashed lines) are: n = 1, Jo = 6.1262×10^{-27} A/cm^2. R_{sheet} for the lateral-conduction layer/LCL (light gray) is varied. All other resistances are negligible. The photocurrent density J_{ph} for the 100 µm x 100 µm illuminated area is 14 A/cm^2. No photocurrent is generated beneath the top contacts (dark gray). A bottom contact (also dark gray) covers the entire bottom surface. $J_z(x)$ in this paper is defined to be the current density through the junction beneath the LCL, where x is the horizontal distance from the top contact. V(x) is the voltage across the junction.

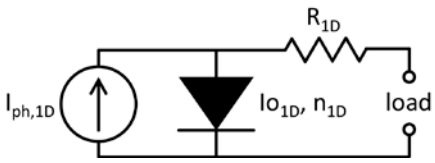

Fig. 2. Equivalent circuit for 1D calculations. $I_{ph,1D}$ = 1.4 mA, n_{1D} = 1, Io_{1D} = 7.35144x10^{-31} A, $R_{1D} = R_{sheet}$ / 12.

been set to negligible values.

In the modeling that follows, R_{sheet} of the LCL will be varied over 13 orders of magnitude without changing any other aspect of the solar cell. Although this may be impossible to duplicate experimentally, modeling makes it possible to look at the full range of R_{sheet} values independent of all other processes. What is essentially being studied are the consequences of lateral voltage variations in the LCL, and these can be caused by high concentration, non-uniform irradiance, large finger spacings and/or high R_{sheet} values. Varying R_{sheet} with the cell size and concentration held constant is simply the easiest configuration for discussion because the incident power remains constant. The model parameters were chosen to approximate the Voc and Jsc values of a $GaInP_2$ cell at 1000 suns concentration. For simplicity, a single diode model with n = 1 has been used. All calculations are at 27 °C.

An equivalent circuit for 1D calculations is shown in Fig. 2. The R_{1D} value of R_{sheet}/12 gives the correct I^2R power loss in the LCL for the low R_{sheet} limit in which the current density $J_z(x)$ flowing normal to the junction is

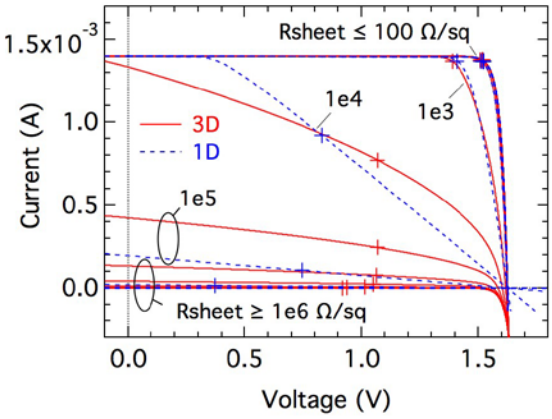

Fig. 3. IV curves for a range of R_{sheet} values computed using 1D and 3D models. The maximum power point of each curve is marked with a "+". The notation "1e*n*" denotes "10^n" (for all figures).

constant (for a square cell with top contacts along two edges). A derivation of R_{1D} can be found in Ref. [10]. $I_{ph,1D}$ is simply J_{ph} multiplied by the *illuminated* area (100 µm x 100 µm), whereas the Io_{1D} value is Jo multiplied by the *total* area (120 µm x 100 µm).

III. Results

The resulting current-voltage (IV) curves are shown in Fig. 3. For low sheet resistance, the 1D model is a good approximation to the more rigorous 3D model. However, for $R_{sheet} \geq 10^3$ Ω/sq, the IV curves for the 1D and 3D models become qualitatively different, indicating a breakdown of the 1D model assumptions.

A close examination of the I-V curves near Voc in Fig. 3 reveals further differences between the 1D and 3D models. For the 3D model, a decrease in Voc occurs when R_{sheet} becomes large (Fig. 4). This is related to the optical opacity of the top contacts. For large R_{sheet}, there is a measurable lateral voltage variation as a small fraction of the photogenerated current flows from the illuminated area to the dark area under each top contact. As can be seen in Fig. 4 (right), this voltage gradient lowers V_{load}. ($Voc_{cell} = V_{load}$ when $I_{load} = 0$.) This effect is inherently a 3D effect, and is therefore not captured by the 1D model.

The powers produced and dissipated by the various elements of the solar cell during operation at its maximum power point (mpp) are plotted in Fig. 5. Four operating regimes have been indicated for the sake of discussion. (In reality, cell operation transitions continuously between these regimes.) In regime I, the 1D model works well because the I^2R losses in the LCL are negligible, but it is rarely possible to make concentrator cells which operate optimally in this regime. At the other extreme, the 1D assumptions completely fail in regime IV, but cells are

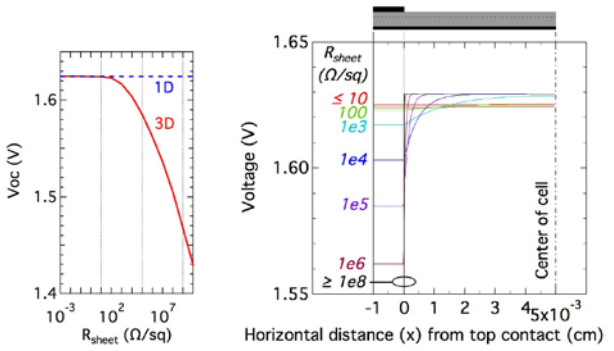

Fig. 4. (left) A Voc drop at large R_{sheet} due to top contact shading is seen for the 3D case, but is absent from the 1D case. (right) V_{diode} at V_{load} = Voc computed using the 3D model. (right, top) Corresponding side view of (half) cell.

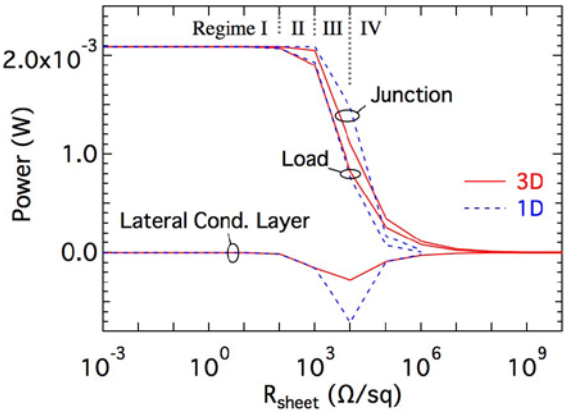

Fig. 5. Power production and dissipation for a range of R_{sheet} values computed using 1D and 3D models at the maximum power point (mpp). The (positive) magnitude of P_{load} is shown here. $P_{junction}$ is the power produced by the junction: $P_{junction} = |P_{load}| + |P_{LCL}|$.

rarely operated in this regime either because very little photocurrent is extracted from the cell (thus the drop in junction power).

Regimes II and III are of far more interest. Typically, a cell will be optimized for operation in regime II, where I^2R losses are the main power loss and the 1D model assumptions are still reasonable. In regime III, losses of junction power are becoming more important than I^2R LCL losses, and the 1D model assumptions are beginning to fail. Nonetheless, solar cells can be operated or characterized in regime III, and the use of a 1D model in this regime can be affected by the failure of the 1D assumptions. For example, 1D and 3D IV curves in regime III can be qualitatively different (see Fig. 3). 3D SPICE modeling may provide additional insight because the internal voltages and currents can be examined in detail, as described below.

IV. Discussion

One of the benefits of cell modeling is that it can provide information about internal processes which is difficult or impossible to measure directly. Figs. 6 and 7 provide information about V(x) and J_z(x) for the idealized cell in Fig. 1. Similar plots for a real cell can be created using a real cell's geometry and parameters, most likely varying a cell dimension or the concentration instead of varying R_{sheet}. The essential features will be the same.

As R_{sheet} (or a cell dimension, or the concentration) increases, the lateral voltage variation between the top contacts and the middle of the cell will increase. However, once the diode voltage at the center of the cell reaches Voc_{diode} (Fig. 6), V(x) cannot increase further.

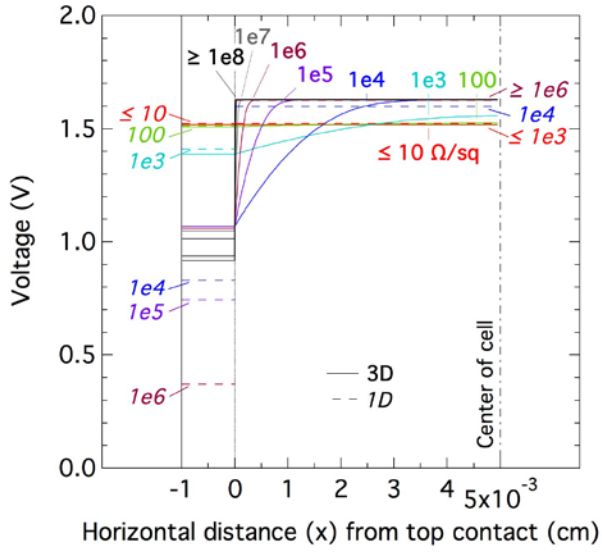

Fig. 6. Solid lines show the diode voltage as a function of position for the 3D model. Because the contact resistance was negligible, V_{diode} under the top contact is equal to V_{load}. Dashed lines show the load voltage (left) and diode voltage (right) for the 1D model. The R_{sheet} values along the left and right sides label the 1D (dashed) lines. All R_{sheet} labels are in Ω/sq. The cell was operated at its maximum power point in all cases.

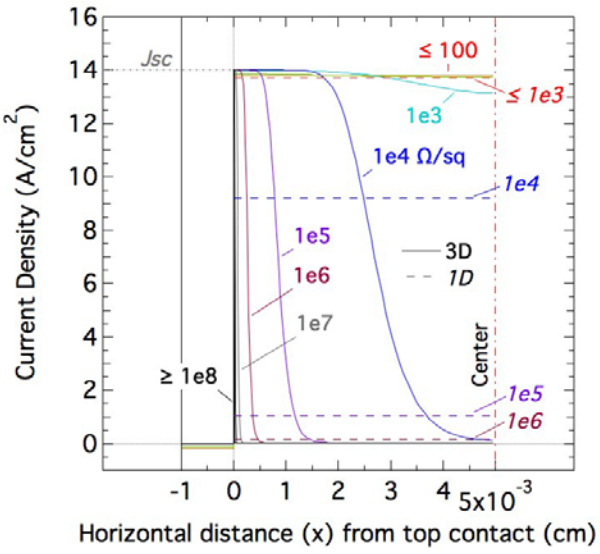

Fig. 7 Solid lines show J_z(x) (current flowing normal to the junction in Fig. 1) computed using the 3D model. All curves are for operation at the maximum power point. Dashed lines show Impp/(100 µm x 100 µm) for the 1D model. The R_{sheet} values along the right side label the 1D (dashed) lines.

Once this happens, further increases in the lateral voltage gradient are obtained by 1) reducing V_{load} and 2) confining the lateral voltage drop to a smaller distance by operating a larger region of the cell near Voc_{diode}. The curves in Fig. 6 indicate that the 1D assumption about constant diode voltage begins to fail as R_{sheet} exceeds 10^3 Ω/sq (for this example).

The $J_z(x)$ curves in Fig. 7 are computed directly from the V(x) curves in Fig. 6 using the diode equation. As the diode voltage at a particular location reaches Voc, the current collected at that location falls to zero. (This corresponds to the sudden drop in junction power for $R_{sheet} > 10^3$ Ω/sq in Fig. 5). The curves in Fig. 7 also indicate that the 1D assumption about constant diode current begins to fail as R_{sheet} exceeds 10^3 Ω/sq (for this example).

A subtle detail in Fig. 7 is that J(x) reaches Jsc for small (positive) values of x as R_{sheet} becomes large. This is because V(x) near the top contact decreases with R_{sheet}, pushing the local operating point toward Jsc. Although this small increase has little effect on power production, an awareness of such subtleties is valuable when interpreting the output generated by 3D modeling of more complicated situations.

V. CONCLUSIONS

Using 3D SPICE-based modeling of a model junction as a function of lateral-conduction-layer sheet resistance, we identified differences between a 3D and 1D model as a cell is pushed into an operating regime where the 1D assumptions of uniform diode voltage and current density begin to fail. Although the cell geometry used in this study was simplified for the purposes of illustration, similar effects are observed during the modeling of more realistic cell geometries.

ACKNOWLEDGMENTS

This work was supported by the U.S. Department of Energy under Contract No. DE-AC36-08-GO28308 with the National Renewable Energy Laboratory. The authors would also like to acknowledge helpful discussions with J.A. Pérez, V. Sabnis and C.D.H. Williams.

REFERENCES

[1] L. W. Nagel, "SPICE2: A Computer Program to Simulate Semiconductor Circuits," EECS Department, University of California, Berkeley, 1975.

[2] K. Nishioka, T. Takamoto, T. Agui, M. Kaneiwa, Y. Uraoka, and T. Fuyuki, "Evaluation of InGaP/InGaAs/Ge Triple-Junction Solar Cell under Concentrated Light by Simulation Program with Integrated Circuit Emphasis," *Japanese Journal of Applied Physics,* vol. 43, p. 882, 2004.

[3] I. Garcia, C. Algora, I. Rey-Stolle, and B. Galiana, "Study of non-uniform light profiles on high concentration III-V solar cells using quasi-3D distributed models," in *Photovoltaic Specialists Conference, 2008. PVSC '08. 33rd IEEE*, 2008, pp. 1-6.

[4] I. Garcia, P. Espinet, I. Rey-Stolle, E. Barrigón, and C. Algora, "Extended Triple-Junction Solar Cell 3D Distributed Model: Application to Chromatic Aberration-Related Losses," in *7th International Conference on Concentrating Photovoltaic Systems*, Las Vegas, NV, 2011.

[5] B. Galiana, C. Algora, and I. Rey-Stolle, "Explanation for the dark I–V curve of III–V concentrator solar cells," *Progress in Photovoltaics: Research and Applications,* vol. 16, pp. 331-338, 2008.

[6] B. Galiana, C. Algora, I. Rey-Stolle, and I. G. Vara, "A 3-D model for concentrator solar cells based on distributed circuit units," *Electron Devices, IEEE Transactions on,* vol. 52, pp. 2552-2558, 2005.

[7] A. Zekry and A. Y. Al-Mazroo, "A distributed SPICE-model of a solar cell," *Electron Devices, IEEE Transactions on,* vol. 43, pp. 691-700, 1996.

[8] A. W. Haas, J. R. Wilcox, J. L. Gray, and R. J. Schwartz, "Numerical modeling of loss mechanisms resulting from the distributed emitter effect in concentrator solar cells," in *Photovoltaic Specialists Conference (PVSC), 2009 34th IEEE*, 2009, pp. 002244-002249.

[9] C. D. H. Williams, "MacSpice 3f5 version 2.10.27," ed, 2010.

[10] A. R. Moore, "An Optimized Grid Design for a Sun-Concentrator Solar Cell," *RCA Review,* vol. 40, pp. 140-152, 1979.